Conference materials
UDC [66.061.16;544.163.2:621.793]:681.586.72
DOI: https://doi.org/10.18721/JPM.163.237

Mechanisms of residual polymer removal in solvent mixtures after the graphene transfer and effects on channel conductivity gate control

N.P. Nekrasov✉, A.V. Romashkin, L.A. Barsukov, K.G. Nikitin, D.D. Levin, I.I. Bobrinetskiy, V.K. Nevolin

National Research University of Electronic Technology, Moscow, Russia

✉ 8141147@gmail.com

Abstract. After graphene transfer, solvent mixtures were used to remove residual PMMA, which efficiency was estimated by AFM, Raman spectroscopy, and CVC. That post-treatment gives: stress relaxation (2D peak shift, compared to trichloroethylene), 2D/G intensity ratio 1.1 changes to 2.6, clean graphene regions exceed 100–150 nm size; threshold point shifts to zero but the conductivity and mobility reduce. Ethanolamine functionalizes both PMMA and graphene.

Keywords: graphene transfer, polymer removal, sensor, polymethyl methacrylate

Funding: This work was supported by Russian Science Foundation, agreement No. 19-19-00401 (development of PMMA removing techniques); grant of the President of the Russian Federation MK-4010.2022.4 (AFM, Raman study).

Citation: Nekrasov N.P., Romashkin A.V., Barsukov L.A., Nikitin K.G., Levin D.D., Bobrinetskiy I.I., Nevolin V.K., Mechanisms of Residual Polymer Removal in Solvent Mixtures after the Graphene Transfer and Effects on Channel Conductivity Gate Control, St. Petersburg State Polytechnical University Journal. Physics and Mathematics. 16 (3.2) (2023) 217–222. DOI: https://doi.org/10.18721/JPM.163.237

Материалы конференции
УДК [66.061.16;544.163.2:621.793]:681.586.72
DOI: https://doi.org/10.18721/JPM.163.237

Механизмы удаления остаточного полимера в смесях растворителей после переноса графена и влияние на проводимость и управление канала

Н.П. Некрасов✉, А.В. Ромашкин, Л.А. Барсуков, К.Г. Никитин, Д.Д. Левин, И.И. Бобринецкий, В.К. Неволин

Национальный исследовательский университет «МИЭТ», Москва, Россия

✉ 8141147@gmail.com

Аннотация. Остаточный ПММА удалялся в смеси растворителей, эффективность оценивали по АСМ, спектроскопии КР и ВАХ. При обработке: напряжения релаксируют (смещение 2D пика); 2D/G меняется: с ~1,1 до 2,6; чистые области становятся 100-150 нм; пороговая точка смещается к нулю, но проводимость и подвижность снижаются. Этаноламин функционализирует и ПММА и графен.

Ключевые слова: перенос графена, сенсор, удаление полимера, ПММА

Финансирование: Работа выполнена в рамках гранта РНФ, № 19-19-00401 (методы удаления полимера); гранта Президента РФ № МК-4010.2022.4 (АСМ и спектроскопия).

Ссылка при цитировании: Некрасов Н.П., Ромашкин А.В., Барсуков Л.А., Никитин К.Г., Левин Д.Д., Бобринецкий И.И., Неволин В.К. Механизмы удаления остаточного полимера в смесях растворителей после переноса графена и влияние на проводимость и управление канала // Научно-технические ведомости СПбГПУ. Физико-математические науки. 2023. Т. 16. № 3.2. С. 217–222. DOI: https://doi.org/10.18721/JPM.163.237

Introduction

The removal of polymer residuals, that are left after the graphene transfer used for the sensor channel, is still an important problem [1]. Residual PMMA blocks the active sensor area and decreases its efficiency, affecting the limit of detection, sensitivity, response time, and sensor parameters reproducibility [2–4]. PMMA tends to strongly interact with graphene in the near-surface layer [5], therefore needs new ways to delete it from graphene, rather than the methods based on bulk material dissolution. We suggest some new methods to remove the near-surface layer using: rinsing in solvent/non-solvent mixture; swelling or functionalization of the PMMA layer. Although the use of mixtures of solvents [6] and some special [1] for removing PMMA, provides a sufficiently high quality of CVD graphene transferred to the target substrate. Nevertheless, some mechanisms for removing PMMA molecules from the graphene and the solvent molecules' interaction with PMMA remain unclear. Despite the use of low molecular weight PMMA and other polymers, plasma modification, etc. [7] the functionalization of residual PMMA with the role of polar side groups increase for its subsequent more efficient removal has not been found in the literature. Thus, the study of the mechanisms of residual PMMA removal from graphene using different solvent mixtures and the PMMA functionalization, as well as graphene characteristics changes as the results of that cleaning, were the goals of this work. The rinsing efficiency and PMMA layer parameters change were estimated by AFM, Raman spectroscopy, and CVC measurements of the graphene layer.

Materials and methods

CVD graphene (Graphenea, Spain) on Cu foil was used. PMMA with M_w ~495 kDa 2 % in anisole (MicroChem, USA) was used as the supporting layer required for transfer onto Si substrate with 300 nm SiO_2 layer with Cr/Au microelectrodes (50 μm gap with 100 μm channel width). PMMA was spin-coated onto graphene at 2.5 krpm, then annealed at 110 °C. To remove polymer residuals film on SiO_2/Si substrate was rinsed in different solvents or mixtures: firstly, trichloroethylene (TCE) at room temperature, and then consequently diacetone alcohol (DAA):water (H_2O) (4:1), tetrahydrofuran (THF):H_2O (Komponent-Reaktiv, Russia) (7:3), ethanolamine (EA) (Sigma-Aldrich):THF (3:7) for half an hour at ~60 °C to increase the dissolution rate. Residual PMMA removing efficiency was investigated using AFM (Solver-Pro, NT-MDT, Russia) and Raman spectroscopy (Centaur U HR, 532 nm laser, Nano Scan Technology, Russia). CVC measurements (IPPP5/1, MNIPI, Belarus) were carried out using a liquid gate (Ag/AgCl in 0.1x PBS 7.0 pH) with PDMS mask with well diameter 700 μm to localize liquid area, drain-source voltage was 10 mV.

Results and Discussion

In comparison with trichloroethylene (TCE), for DAA:H_2O there is stress relaxation or doping (2D peak shifts from 2696 to 2690 cm^{-1}), but with no 2D/G ratio change (~1.1, Fig. 1), although the layer thickness increased (from 3.7 to 4 nm, Fig. 2, *a*, *c*). This behavior can be explained by polymer swelling in the solvent with polymer molecular chain conformations changing relative to each other and graphene. That leads to the stress relaxation formed before: during the graphene transfer with an initially continuous PMMA layer and their heat treatment on the substrate. However, such PMMA swelling is not enough to redistribute PMMA molecules and remove them from graphene. Increasing solvent temperature potentially can improve PMMA removal efficiency. But used temperature already results in the graphene being partially removed from SiO_2, which appears as the curled edge of the graphene layer with residual PMMA (Fig. 2,*c*). Thus, due to the more energy-favorable PMMA-graphene interaction compared to PMMA-PMMA,

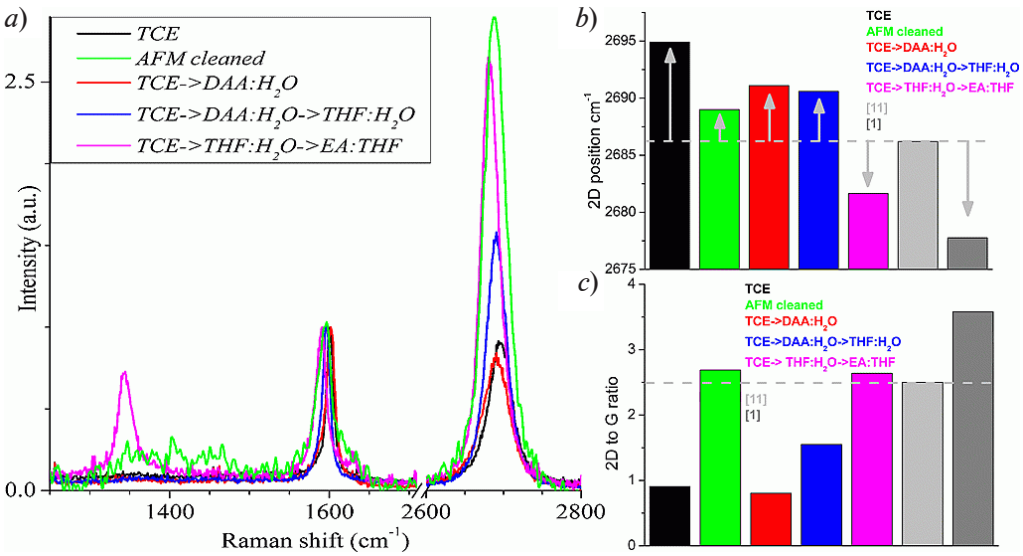

Fig. 1. Raman spectra (*a*), 2D position (*b*), 2D/G peak ratio (*c*) of graphene rinsed in various solvents

instead of easy removal of PMMA in TCE, which is one of the best solvents for PMMA [8], the removal of the near-surface PMMA layer from graphene does not occur. And as the temperature increases, only the graphene removal along with the residual PMMA layer occurs, especially if a large part of graphene was covered by PMMA. Thus, a two-stage treatment was carried out: (i) the main PMMA layer thickness was gradually removed in TCE at 25 °C, (ii) the residual near-surface PMMA layer was removed in a solvents mixture not exceed 60 °C.

For THF:H_2O, 2D/G increases to 1.6-1.9, which with AFM data (thickness ~2.2 nm), indicates that graphene regions without PMMA increased to ~50 nm. In our previous work [9], similar processing led to the graphene areas formation on Cu foil, on the contrary, with residual PMMA on that areas with slightly smaller sizes, with fluorescence from such quantum dots. In current work also small graphene regions, but without PMMA, don't provide fluorescence on SiO_2, but also suppress 2D/G. Due to its small specific area contribution, they can't change 2D/G ratio in the case of TCE compared to full PMMA-covered graphene. If its contribution and at the same time its size would be larger, 2D/G should be ~5 [9]. Graphene regions contribution, locally with high quality (2D/G ~5 [1, 9]), could be suppressed by the larger proportion of areas with PMMA (2D/G ~1) that total contribution is more than 2/3 of the whole area (Fig. 2,*d*).

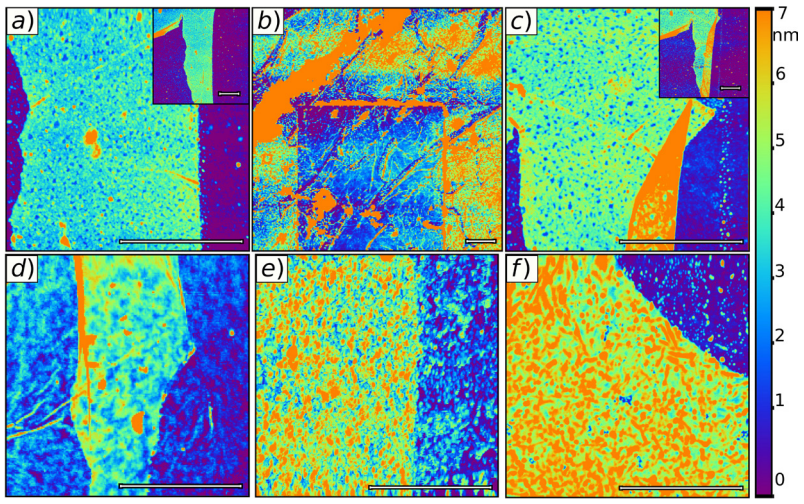

Fig. 2. AFM of graphene cleaned by: TCE (*a*), AFM (*b*), DAA:H_2O (*c*), THF:H_2O (*d, e*), (*e*) correspond to another sample, EA:THF (*f*). Scale bars are 1 μm

At the same time, with a small size of such small islands of graphene with PMMA or, similarly, without PMMA limited by PMMA, due to the possibility of fluorescence in them on copper foil [9], the energy levels position can also significantly change for them, even in the case of graphene on SiO_2, accompanied by significant suppression of the 2D intensity for such regions. Thus, even in the presence of a large proportion of graphene without PMMA, the 2D/G ratio will be significantly suppressed when the regions with and without PMMA are small in size. Observed changes in the shape and area of the graphene regions without PMMA when using THF, points to the redistribution and only partial PMMA removal, especially on SiO_2 at an increased annealing temperature after transfer.

2D/G of AFM-cleaned graphene was higher: ~2.7. The thickness of the graphene layer is still larger (0.7–1 nm) than that observed for exfoliated graphene, transferred without polymers and solvents. The increased thickness is associated with the residual water molecules on SiO_2 under graphene for PMMA-transferred CVD graphene [10]. A further 2D/G ratio increase in comparison with the AFM-cleaned graphene is possible using a different substrate containing fewer residual water molecules and functional groups (such as Si-OH) on the surface or with special cleaning of the substrates [1]. Similar is realized for exfoliated graphene, which interacts weakly with an underlying graphene sublayer separating the upper layer from SiO_2, in comparison with the graphene directly on SiO_2 [11]. The decrease in 2D/G is due to the formation of graphene regions with different types and charge densities [12]. It leads to a broadening and, accordingly, a 2D peak intensity decrease. That is a result of the graphene interaction with a similar substrate in our case also containing regions with different potential.

For EA:THF, the 2D peak is shifted from 2690 to 2681 cm^{-1} and 2D/G increases to 2.6 which points to extended graphene regions without PMMA. Therefore, EA functionalization of PMMA helps to remove PMMA, but graphene is functionalized too (D/G~0.7). Although the AFM thickness is ~5 nm. The ethanolamine functionalization of PMMA [13] makes it capable of retaining a sufficient number of solvent and H_2O molecules [14]. That forms the effective layer thickness increase. Additionally, graphene functionalization also occurs, which is specific, without long-term heat treatment and catalyzing agents [15]. A possible explanation for the graphene functionalization is the formation of reactive radicals during the PMMA functionalization, which as a result leads, together with ethanolamine, to the graphene functionalization. Such modification is not acceptable for some sensors.

Despite the PMMA partial removal with the 2D/G increasing (>1.5 is considered acceptable [2]) and the threshold point shifting to zero (Fig. 3), the conductivity and mobility decrease. That is explained by the formation of alternating regions with (~30–60 % of the surface) and without PMMA along the channel after THF:water cleaning, which differs in properties. The alternating can even reduce the CVC slope (Fig. 2,*d*, 3, *a*, *b*) in contrast to TCE cleaning, and to some known results. Although the AFM probe partially removes most of the PMMA from the graphene and shifts the threshold point closer to zero. Nevertheless, it does not lead to a significant increase in the CVC slope [16], in comparison with graphene purified by more efficient methods [1]. Thus even a small PMMA residual amount reduces the CVC slope.

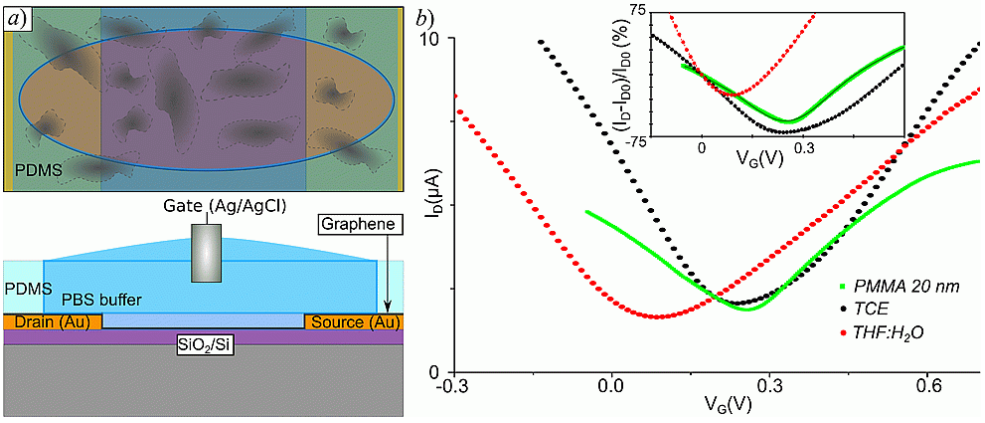

Fig. 3. CVC measuring scheme (*a*), CVC (*b*) of initial graphene with PMMA and rinsed in solvents and the inset is the I_D changes relative to I_{D0} depending on V_G, where I_{D0} is $I_D(V_G = 0\ V)$

Hole mobility was estimated from CVC slope using a simple field-effect transistor equation: $\mu_h = [(\Delta I_D/\Delta V_G)(L/W)]/(C_{ox}/V_D)$, where L, W are the channel length and width; $C_{ox} = 5$ μF/cm^2 is the gate electrolyte double-layer specific capacitance [17–19]. The estimated μ_h for different structures are: 107 cm^2/Vs for PMMA covered, 249 cm^2/Vs for TCE, 202 cm^2/Vs for THF:H_2O. Significant μ_h decrease for graphene cleaned by THF:H_2O can be explained by the integrity destruction of the PMMA layer, remained after TCE, with the formation of an island character of the residual PMMA layer (Fig. 2,*a*, *d*). These graphene regions' alternation with and without polar groups of PMMA molecules can form charge density level or even conductivity type differences along the channel. It can significantly reduce gate control [20, 12]. Nevertheless, the I_D change relative to I_{D0} depending on V_G has a higher slope than for TCE (Fig. 3,*b*, inset), so the THF:H_2O cleaned graphene resistive sensor has potentially higher sensitivity.

Conclusions

Trichloroethylene (TCE) cannot remove the near-surface PMMA layer. In comparison with TCE, for DAA:water there are: stress relaxation (2D peak shifts) with layer thickness increased due to swelling, but no 2D/G ratio change (~1.1). Also, graphene was partially removed due to the solvent high temperature (60 °C) while maintaining a high interaction energy of the remaining PMMA layer with graphene. For tetrahydrofuran (THF):water treatment, 2D/G increases to 1.6-1.9, and graphene regions without PMMA increase to ~50 nm and more. And according to AFM, redistributed PMMA still occupies about half of the graphene surface. 2D/G of AFM cleaned graphene was higher: ~2.7 which is consistent with pure graphene Raman data. Although at AFM PMMA remains in several regions. Thus, the graphene cleaning control only by Raman is not enough, AFM is required. For ethanolamine (EA):THF, the 2D peak is shifted and 2D/G is 2.6 which points to extended graphene regions without PMMA. Although the AFM thickness is ~5 nm due to swelling. Thus, EA functionalization helps to remove PMMA, but graphene is functionalized too (D/G~0.7). Despite the PMMA partial removal after THF:water treatment with the 2D/G increasing and the threshold point shifting to zero, the conductivity and mobility decrease. The alternating of with and without PMMA regions forms different charge density levels or even conductivity types along the channel, which in turn significantly reduces channel control from the gate. Nevertheless, such resistive sensors might have better sensitivity.

REFERENCES

1. **Tyagi A., Mišeikis V., Martini L., Forti S., Mishra N., Gebeyehu Z. M., Giambra M. A., Zribi J., Frégnaux M., Aureau D., Romagnoli M., Beltram F., Coletti C.** Ultra-clean high-mobility graphene on technologically relevant substrates, Nanoscale. 14 (6) (2022) 2167–2176.

2. **Nekrasov N., Jaric S., Kireev D., Emelianov A. V., Orlov A. V., Gadjanski I., Nikitin P. I., Akinwande D., Bobrinetskiy I.,** Real-time detection of ochratoxin A in wine through insight of aptamer conformation in conjunction with graphene field-effect transistor, Biosensors and Bioelectronics. 200 (2021) 113890.

3. **Romashkin A. V., Struchkov N. S., Lashkov A. V., Shpakov D. S., Nekrasov N. P., Emelianov A. V.** Ammonia Recognition at Different Humidity with a Graphene Sensors Array Modified by a Focused Ion Beam. Proceedings of the 2022 International Conference on Actual Problems of Electron Devices Engineering, Saratov, IEEE, (2022) 186–190.

4. **Hong J., Lee S., Seo J., Pyo S., Kim J., Lee T.,** A highly sensitive hydrogen sensor with gas selectivity using a PMMA membrane-coated Pd nanoparticle/single-layer graphene hybrid, ACS applied materials & interfaces. 7(6) (2015) 3554–3561.

5. **An R., Huang L., Mineart K. P., Dong Y., Spontak R. J., Gubbins K. E.,** Adhesion and friction in polymer films on solid substrates: conformal sites analysis and corresponding surface measurements, Soft Matter. 13(19) (2017) 3492–3505.

6. **Miller-Chou B. A., Koenig J. L.,** A review of polymer dissolution, Progress in Polymer Science 28(8) (2003) 1223–1270.

7. **Zhuang B., Li S., Li S., Yin J.,** Ways to eliminate PMMA residues on graphene – superclean graphene, Carbon. 173 (2021) 609–636.

8. **Evchuk I. Y., Musii R. I., Makitra R. G., Pristanskii R. E.,** Solubility of polymethyl methacrylate in organic solvents, Russian journal of applied chemistry. 78 (10) (2005) 1576–1580.

9. **Barsukov L. A., Nekrasov N. P., Romashkin A. V., Bobrinetskiy I. I., Levin D. D., Nevolin V. K.,** Improved polymer residuals removing after the graphene transfer to enhance sensors performance, St. Petersburg State Polytechnical University Journal. Physics and Mathematics. 16 (1.3) (2023) 44–49.

10. **Bobrinetskiy I., Emelianov A., Nasibulin A., Komarov I., Otero N., Romero P. M.,** Photophysical and photochemical effects in ultrafast laser patterning of CVD graphene, Journal of Physics D: Applied Physics. 49(41) (2016) 41LT01.

11. **Ferrari A. C., Basko D. M.,** Raman spectroscopy as a versatile tool for studying the properties of graphene, Nature nanotechnology. 8 (4) (2013) 235–246.

12. **Martin J., Akerman N., Ulbricht G., Lohmann T., Smet J. V., Von Klitzing K., Yacoby A.,** Observation of electron–hole puddles in graphene using a scanning single-electron transistor, Nature physics. 4(2) (2008) 144–148.

13. **Yu Y., Brown G. R.,** Carbon-13 NMR study of the kinetics of the functionalization of poly (methyl acrylate) by reaction with ethanolamine, Macromolecules. 25(24) (1992) 6658–6663.

14. **Lewis C. L., Anthamatten M.,** Synthesis, swelling behavior, and viscoelastic properties of functional poly (hydroxyethyl methacrylate) with ureidopyrimidinone side-groups. Soft Matter, 9 (15) (2013) 4058–4066.

15. **Dao T. D., Hong J. E., Ryu K. S., Jeong H. M.,** Super-tough functionalized graphene paper as a high-capacity anode for lithium ion batteries, Chemical Engineering Journal. 250 (2014) 257–266.

16. **Choi W., Shehzad M. A., Park S., Seo Y.,** Influence of removing PMMA residues on surface of CVD graphene using a contact-mode atomic force microscope, RSC advances. 7(12) (2017) 6943–6949.

17. **Ruslinda A. R., Tanabe K., Ibori S., Wang X., Kawarada H.,** Effects of diamond-FET-based RNA aptamer sensing for detection of real sample of HIV-1 Tat protein. Biosensors and Bioelectronics, 40 (1) (2013) 277–282.

18. **Takagi S. I., Toriumi A.,** Quantitative understanding of inversion-layer capacitance in Si MOSFET's. IEEE Transactions on Electron Devices, 42 (12) (1995) 2125–2130.

19. **Chen P. W., Tseng C. Y., Shi F., Bi B., Lo Y. H.,** Measuring electric charge and molecular coverage on electrode surface from transient induced molecular electronic signal (TIMES). Scientific reports, 9(1) (2019) 1–10.

20. **Zhang Y., Yuan Y., Cao G., Han C., Li X., Wang X., Zhang G., Geng Li, Liu W.,** A fresh-bias photoresponse of graphene field-effect transistor: An electrical tunable fast dipole moment generation, Carbon. 173 (2021) 322–328.

THE AUTHORS

NEKRASOV Nikita P.
8141147@gmail.com
ORCID: 0000-0003-1417-0177

BARSUKOV Leonty A.
leonty.barsukov@gmail.com
ORCID: 0000-0002-4802-0014

LEVIN Denis D.
skaldd@yandex.ru
ORCID: 0000-0002-8414-6191

NEVOLIN Vladimir K.
vkn@miee.ru
ORCID: 0000-0003-4348-0377

ROMASHKIN Alexey V.
romaleval@gmail.com
ORCID: 0000-0002-0101-6122

NIKITIN Konstantin G.
halkwww@mail.ru
ORCID: 0000-0002-0457-4568

BOBRINETSKIY Ivan I.
bobrinet@mail.ru
ORCID: 0000-0003-2380-2594

Received 05.07.2023. Approved after reviewing 24.08.2023. Accepted 26.08.2023.